frontiers in Physiology

ORIGINAL RESEARCH
published: 13 December 2017
doi: 10.3389/fphys.2017.01053

Nitrite-Mediated Hypoxic Vasodilation Predicted from Mathematical Modeling and Quantified from *in Vivo* Studies in Rat Mesentery

Donald G. Buerk, Yien Liu, Kelly A. Zaccheo, Kenneth A. Barbee and Dov Jaron*

School of Biomedical Engineering, Science and Health Systems, Drexel University, Philadelphia, PA, United States

Nitric oxide (NO) generated from nitrite through nitrite reductase activity in red blood cells has been proposed to play a major role in hypoxic vasodilation. However, we have previously predicted from mathematical modeling that much more NO can be derived from tissue nitrite reductase activity than from red blood cell nitrite reductase activity. Evidence in the literature suggests that tissue nitrite reductase activity is associated with xanthine oxidoreductase (XOR) and/or aldehyde oxidoreductase (AOR). We investigated the role of XOR and AOR in nitrite-mediated vasodilation from computer simulations and from *in vivo* exteriorized rat mesentery experiments. Vasodilation responses to nitrite in the superfusion medium bathing the mesentery equilibrated with 5% O_2 (normoxia) or zero O_2 (hypoxia) at either normal or acidic pH were quantified. Experiments were also conducted following intraperitoneal (IP) injection of nitrite before and after inhibiting XOR with allopurinol or inhibiting AOR with raloxifene. Computer simulations for NO and O_2 transport using reaction parameters reported in the literature were also conducted to predict nitrite-dependent NO production from XOR and AOR activity as a function of nitrite concentration, PO_2 and pH. Experimentally, the largest arteriolar responses were found with nitrite >10 mM in the superfusate, but no statistically significant differences were found with hypoxic and acidic conditions in the superfusate. Nitrite-mediated vasodilation with IP nitrite injections was reduced or abolished after inhibiting XOR with allopurinol ($p < 0.001$). Responses to IP nitrite before and after inhibiting AOR with raloxifene were not as consistent. Our mathematical model predicts that under certain conditions, XOR and AOR nitrite reductase activity in tissue can significantly elevate smooth muscle cell NO and can serve as a compensatory pathway when endothelial NO production is limited by hypoxic conditions. Our theoretical and experimental results provide further evidence for a role of tissue nitrite reductases to contribute additional NO to compensate for reduced NO production by endothelial nitric oxide synthase during hypoxia. Our mathematical model demonstrates that under extreme hypoxic conditions with acidic pH, endogenous nitrite levels alone can be sufficient for a functionally significant increase in NO bioavailability. However, these conditions are difficult to achieve experimentally.

Keywords: aldehyde oxidoreductase, allopurinol, hypoxic vasodilation, nitrite reductases, nitric oxide, raloxifene, xanthine oxidoreductase

OPEN ACCESS

Edited by:
Joseph M. Rifkind, Johns Hopkins University, United States

Reviewed by:
Charles Dionisio Eggleton, University of Maryland, Baltimore County, United States
Rolando Juan Jose Ramirez, University of Akron, United States

****Correspondence:***
Donald G. Buerk
donald.gene.buerk@drexel.edu

Specialty section:
This article was submitted to Vascular Physiology, a section of the journal Frontiers in Physiology

Received: *27 September 2017*
Accepted: *01 December 2017*
Published: *13 December 2017*

Citation:
Buerk DG, Liu Y, Zaccheo KA, Barbee KA and Jaron D (2017) Nitrite-Mediated Hypoxic Vasodilation Predicted from Mathematical Modeling and Quantified from in Vivo Studies in Rat Mesentery. Front. Physiol. 8:1053. doi: 10.3389/fphys.2017.01053

INTRODUCTION

The primary source of the nitrite anion (NO_2^-) in mammalian systems is from the oxidation of nitric oxide (NO) produced by the L-arginine/NO enzymatic pathway in vascular endothelium by the O_2-dependent endothelial isoform of NO synthase (eNOS). Although physiological effects of nitrite on the cardiovascular system have been known since 1880 (Reichert and Mitchell, 1880), the consensus view had been that nitrite is an inert byproduct of NO production. This viewpoint has changed radically in the past few decades with the emergence of abundant evidence that nitrite serves as a reversible storage reservoir for NO, which can restore NO bioavailability under certain physiological conditions. However, the mechanisms for recovering NO from nitrite are incompletely understood since the biochemical formation of NO metabolic byproducts and regulation of NO bioavailability is complex (Kim-Shapiro and Gladwin, 2014; Blood, 2017; Helms et al., 2017). Furthermore, the accurate measurement of nitrite and related nitrogen species in blood and tissue is technically difficult (MacArthur et al., 2007).

Infusion of sodium nitrite ($NaNO_2$) into the bloodstream has been shown to cause vasodilation in humans, presumably due to conversion of nitrite to NO (Cosby et al., 2003; Dejam et al., 2007; Pluta et al., 2011). Evidence that inorganic nitrite anion therapy may have therapeutic effects for numerous pathological conditions, especially for treating cardiovascular disease, has been reviewed (Kevil et al., 2011; Omar et al., 2016; Blood, 2017), along with substantial experimental evidence for a protective effect from ischemia-reperfusion injury (e.g., see Table 1 in Blood, 2017). Pluta et al. (2011) report that 48 h of continuous IV infusion of $NaNO_2$ is well tolerated in humans, with a maximal tolerable dose of 267 μg/kg/hr. Three of the 12 subjects in this clinical study showed some toxicity at doses of 445.7 μg/kg/hr with a significant decrease in mean arterial blood pressure by more than 15 mmHg in two subjects, and in one subject the methemoglobin level exceeded 5%. Earlier studies using much higher doses of nitrite reported incidences of severe hypotension and lethal methemoglobinemia (Weiss et al., 1937; Wilkins et al., 1937), which curtailed further interest in therapeutic applications for decades. Despite these observed negative effects, nitrite is an approved therapeutic antidote for cyanide and hydrogen sulfide poisoning (Lloyd, 1957; Smith and Gosselin, 1979). More recently, interest in using nitrite for therapeutic purposes has been resurrected. A search of clinicaltrials.gov using nitrite as a keyword presently lists 48 clinical trials that include nitrite as the study drug. Many more dietary studies evaluating the effect of oral nitrate supplements are also listed.

NO generated from nitrite through the deoxyhemoglobin nitrite reductase pathway in red blood cells (RBCs) is proposed to play a major role in hypoxic vasodilation (Gladwin, 2008; Gladwin et al., 2009). However, our previous mathematical model (Buerk et al., 2011a) for coupled NO and O_2 transport around an arteriole predicted that only negligible amounts of NO could reach smooth muscle cells (SMC) in the vascular wall due to very strong scavenging of NO by hemoglobin (Hb) in RBCs. Azizi et al. (2005) used the analogy that the RBC is a "black hole" for NO—it can get in but can't get out. Our previous mathematical model predicted that substantially more NO could be derived from nitrite reductase activity in tissue compared with the deoxyhemoglobin nitrite reductase pathway (Buerk et al., 2011a). Our model prediction for the minor contribution of NO from the deoxyhemoglobin nitrite reductase pathway is consistent with a mathematical model by another group (Chen et al., 2008), which predicted that only picomolar levels of NO could be delivered to vascular SMC. Buerk et al. (2011b) has reviewed other mathematical modeling predictions and relevant experimental data in the literature with respect to several signaling pathways in the microcirculation that involve NO. In general, we found that mathematical predictions for NO values are often lower than reported from experimental measurements, and that very few models developed by other investigators include both the O_2-dependance of NO production from eNOS and the inhibitory effect of NO on O_2 consumption in tissue (coupled NO and O_2 transport), which we always include in our models.

More recently, we developed an alternative deoxyhemoglobin nitrite reductase model to investigate whether dinitrogen trioxide (N_2O_3) can act as a stable intermediate to preserve NO (Liu Y. et al., 2016). The model is based on the assumption that N_2O_3 does not react in the bloodstream (Basu et al., 2007; Hopmann et al., 2011) and will only release NO after it homolyzes in tissue (Butler and Ridd, 2004). Our alterative model predicts that NO is rapidly released from RBC-generated N_2O_3 after it leaves the bloodstream, primarily in the endothelium, with a resulting increase in SMC NO in the vascular wall (Liu Y. et al., 2016). Furthermore, this reaction is enhanced at low blood PO_2 and increases with acidic pH.

We did not include generation of NO by tissue nitrite reductase activity in our recent model (Liu Y. et al., 2016), since we were examining a theoretical mechanism that could spare NO generated in RBCs from strong scavenging by Hb. However, tissue nitrite reductase activity is hypothesized to be a significant source of NO, especially during hypoxia. Both *in vitro* and *in vivo* studies demonstrate that NO generation from nitrite in tissue is associated with the molybdoenzymes xanthine oxidoreductase (XOR) and aldehyde oxidoreductase (AOR) (Li et al., 2008; Webb et al., 2008; Golwala et al., 2009). For the present report, we conducted experiments to test the hypothesis that tissue nitrite reductases increase NO bioavailability and modulate vascular tone of arterioles (20–80 μm diameter range) in the rat mesentery microvasculature under varying PO_2 and pH conditions. We also modified our previous mathematical models (Buerk et al., 2011a; Liu Y. et al., 2016) using available reaction kinetic parameters in the literature for the tissue nitrite reductases XOR and AOR (Maia and Moura, 2011; Maia et al., 2015) to predict NO changes in arteriolar SMC as a function of nitrite concentration, PO_2 and pH.

METHODS

Animals and Animal Care

All animals received humane care according to the criteria outlined in the Guide for the Care and Use of Laboratory Animals prepared by the National Academy of Sciences and published by the National Institutes of Health. All animal protocols were

approved by the Institutional Animal Care and Use Committee at Drexel University. Every effort was made to minimize animal pain and suffering. Male Sprague-Dawley rats (250–300 g, aged 8 weeks) were kept one or two per cage in a temperature-controlled room at 28°C (thermoneutrality for rats) under a 12-h light/12-h dark cycle. All male subjects were used to avoid confounding effects of estrogen on eNOS.

In Vivo Microcirculation Studies

Exteriorized rat mesentery experiments were conducted under isoflurane anesthesia to measure perivascular NO with recessed microelectrodes, arteriolar diameter (D) from video imaging (Neild, 1989) (DiamTrak software purchased from Dr. T.O. Neild, Flinders Univ., Adelaide, Australia), tissue perfusion (relative volumetric RBC flow in capillaries; Bonner et al., 1981) by laser Doppler (LDF, Transonic model BLF22, Ithaca, NY), and small artery (∼270 micron diameter) blood flow with an ultrasonic probe (Transonic model 420, Ithaca, NY). All physiological signals were sampled at 10 Hz with 12-bit accuracy using a computer-controlled data acquisition system. The DiamTrak output was filtered to remove occasional out of range artifacts using Excel, and smoothed with a running average filter. Arteriolar vasodilation was quantified in response to $NaNO_2$ in the superfusion medium (Krebs-ringer bicarbonate buffer) bathing the mesentery equilibrated with either 5% or 10% O_2 and 5% CO_2 (normoxic solution) or zero O_2 (95% N_2) and 5% CO_2 (hypoxic solution) at normal (pH = 7.4) or acidic pH (range 6.5–6.7) and maintained at 37°C. Typically, paired measurements were made for each arteriole, alternating $NaNO_2$ exposures between normoxic or hypoxic solutions. The concentration of $NaNO_2$ in the superfusate was varied up to 25 mM, exposing the preparation to $NaNO_2$ for only short periods of time (typically 3 min duration).

In addition, some superfusion experiments were conducted to quantify arteriolar responses before and after inhibiting XOR with the pyrazolopyrimidine-based inhibitor allopurinol (3.4–6 mg/kg IP). Allopurinol dissolved in normal saline was delivered by a single intraperitoneal (IP) injection through a tube inserted into the abdominal cavity. In addition to $NaNO_2$ exposures in the superfusion solution, *in vivo* experiments were also conducted with measurements taken after an acute IP injection of 3–6 mg/kg mg of $NaNO_2$ while the mesentery was superfused with hypoxic solution at pH = 7.4. After recording control measurements for 3–4 arterioles, XOR oxidase was inhibited with allopurinol and measurements were repeated for the same arterioles. We also conducted studies using either superfusion or an acute IP injection of $NaNO_2$ before and after inhibiting AOR with the estrogen receptor antagonist raloxifene (2.9–10 mg/kg IP).

Mathematical Model

NO and O_2 transport were simulated in a microcirculatory arteriole and surrounding tissue model and solved for steady state conditions using finite element method numerical methods (COMSOL v5.3, Burlington, MA). Coupled non-linear partial differential equations for mass transport were written in cylindrical coordinates including the sum of reactions (R_i) for all chemical species ($C_i = O_2$, NO, NO_2^-)

$$\nabla \cdot (D_i \nabla C_i) - v \nabla C_i \pm \sum R_i = 0 \tag{1}$$

as detailed in our previous modeling efforts (Buerk et al., 2003, 2011a; Lamkin-Kennard et al., 2004a,b; Chen et al., 2006; Chen X. et al., 2007; Liu et al., 2017), where D_i is the diffusion coefficient for each species, and v is the fluid velocity profile in the lumen (assumed to be parabolic).

The model has five concentric cylindrical layers: (i) RBC core, radius = 13 μm, (ii) RBC-free plasma layer, 13 < r < 14 μm, width = 1 μm, (iii) endothelium, 14 < r < 15 μm, width = 1 μm, (iv) vascular wall smooth muscle cell (SMC) layer, 15 < r < 25 μm, width = 10 μm, and (v) perivascular tissue, 25 < r < 130 μm, width = 105 μm. Each layer was assumed to have homogenous properties with uniformly distributed reactions. Both convective and diffusive mass transports are included in the vessel lumen, with only diffusive transport in tissue. NO is produced in the endothelium by eNOS, and generated from nitrite in tissue by either XOR or AOR, or in blood from conversion of nitrite to N_2O_3 (Basu et al., 2007) by Hb in RBCs, with subsequent homolysis to release NO. The model includes O_2-dependent NO production by eNOS, and inhibition of O_2 consumption by NO, using parameters as described for one of our previous models (Chen et al., 2006). The present model now includes reactions for nitrite in blood or tissue, which are compared to a baseline simulation without XOR or AOR.

We modeled the reaction of nitrite with Hb in the bloodstream as

$$\frac{d[NO]}{dt} = k_N \left[Hb\right] [NO_2^-] \tag{2}$$

where the bimolecular rate constant k_N was characterized as a function of blood PO_2 using a modified Monod-Wyman-Changeux (MWC) model of allostery for the oxyhemoglobin equilibrium curve, as described by Rong et al. (2013a,b). We further modified this model (Liu Y. et al., 2016), adding the production of N_2O_3 from NO and nitrite-methemoglobin, catalyzed by the nitrous anhydrase activity of deoxyHb. The O_2-dependent function for k_N in Equation (2) and the complete model parameters used in our simulation are summarized in Liu Y. et al. (2016).

In tissue, the reaction rate for nitrite reduction by XOR was characterized using a Michaelis-Menten equation with competitive inhibition by O_2:

$$v_{Nitrite\ Reduction} = \frac{k_{cat}\left[NO_2^-\right][XOR]}{K_m NO_2^- \left(1 + \frac{[O_2]}{K_m O_2}\right) + [NO_2^-]} \tag{3}$$

where the reaction parameters k_{cat}, $K_m NO_2^-$, and $K_m O_2$ vary depending on tissue pH values (Li et al., 2008; Maia and Moura, 2011; Maia et al., 2015; see **Table 1**). XOR was assumed to be uniformly distributed in the endothelium, SMC layer, and perivascular tissue (Ray and Shah, 2005). Blood PO_2 was varied between normoxic conditions (90 Torr) down to hypoxic

TABLE 1 | Physical parameters and rate constants used in the simulation.

Parameter	Value(s)	References
Tissue nitrite	0–300 μM	
Nitrite diffusion coefficient	410 $\mu m^2/s$	Pinotti et al., 2002; Li et al., 2008; Kim-Shapiro and Gladwin, 2014
XOR concentration		
Heart	0.03 μM	
Liver	0.3 μM	
Reaction parameters at pH = 7.4		Maia and Moura, 2011; Maia et al., 2015
k_{cat}	0.545 s^{-1}	
$K_m NO_2^-$	1918 μM	
$K_m O_2$	24.3 μM	
at pH = 6.3		
k_{cat}	0.581 s^{-1}	
$K_m NO_2^-$	251 μM	
$K_m O_2$	24.3 μM	

levels (10 Torr). Simulations were performed with tissue XOR concentrations ranging between 0.03 and 0.3 μM as found in heart and liver, respectively, where tissue nitrite reduction has been shown to produce a functionally significant elevation in NO (Kim-Shapiro and Gladwin, 2014). The nitrite anion was assumed to be uniformly distributed in all perivascular tissue regions. Simulations were performed with nitrite varying between physiological (<2 μM; Li et al., 2008; van Faassen et al., 2010) to elevated (300 μM) concentrations. Simulations were solved at steady state with a relative tolerance for convergence of 0.001 and an absolute tolerance of 0.0001. The initial mesh for the computational domain consisted of 19,976 domain elements and 1,678 boundary elements. Meshing was calibrated such that further refinement did not change predicted NO concentration more than 0.01 nM.

RESULTS

The presence of $NaNO_2$ in the superfusion medium usually elicited vasodilatory responses for the arterioles observed in this study, consistent with an increase in NO bioavailability. In a few cases, no change or minor vasoconstriction was observed. However, we were not able to accurately measure perivascular tissue NO due to electrochemical interference with nitrite at the high concentrations used in our superfusion experiments. Quantitative results using superfusion protocols are summarized in **Figure 1** for several individual experiments using short exposures to $NaNO_2$ (typically 3 min duration, indicated by striped bars). There were approximately 30 s transport delays from the time when the superfusion pump was switched between reservoirs at $t = 0$ to the time that changes in concentration reached the tissue. The transport delay was determined by observing the time for a bubble introduced at the inlet to emerge at the outlet of the tubing. Representative changes in arteriolar diameter (ΔD) are shown in **Figure 1A** with average responses for 6–7 arterioles from 1 rat experiment, demonstrating enhanced vasodilation with hypoxic conditions in the superfusate. Initial diameters ± SE are indicated. Greater vasodilation responses to $NaNO_2$ were often, but not always, observed using hypoxic solutions with acidic pH compared with hypoxic solutions at normal pH = 7.4. An example from 1 rat experiment with averaged measurements from 6 arteriole pairs is shown in **Figure 1B**. Note that the time rate of diameter change (ΔD/Δt, dashed lines) during the period of $NaNO_2$ superfusion was 38% faster in the acidic solution (0.759 μm/min) compared with the rate of increase at pH = 7.4 (0.55 μm/min) that occurred following a transient decrease in ΔD for this experiment. This transient may reflect a decrease in NO during the period of hypoxic superfusion preceding the exposure to $NaNO_2$. We also recorded the laser Doppler signal (LDF), which is proportional to capillary blood flow and reported with arbitrary tissue perfusion units (tpu). For the example shown in **Figure 1C**, the average change (ΔLDF) during $NaNO_2$ superfusion was negligible when the superfusate pH = 7.4 (open circles). There were increases in capillary blood flow during $NaNO_2$ superfusion with acidic pH (**Figure 1C**, solid circles), although the difference compared with normal pH was not statistically significant. Overall results for the average ΔD ± SE for 44 paired arterioles from $n = 9$ rats are shown in **Figure 1D** for $NaNO_2$ concentrations ranging between 4 and 24 mM in hypoxic superfusion solution. The average ± SE initial diameter was $D_{initial} = 43.4 \pm 1.6$ μm for these measurements. Note that there were many experiments (4/9) where the average increase in ΔD with $NaNO_2$ in acidic superfusion solution was smaller compared to superfusion solutions at normal pH. In three experiments, the average D was slightly negative (no increase in D for two experiments with pH = 7.4 and one experiment for acidic pH). Consequently, there was no statistically significant difference in ΔD determined during $NaNO_2$ superfusion with normal or acidic pH (Mann–Whitney Rank Sum test).

Evidence for the role of XOR was found by comparing vascular responses before and after treating animals with allopurinol (3.4–6 mg/kg IP). Results for the average ΔD with hypoxia and $NaNO_2$ in the 10–12 mM range for three rat experiments is shown in **Figure 2A**, demonstrating a significant reduction in the vasodilatory response after allopurinol (solid circles) compared to control measurements (open circles). The small artery blood flow (BF) to the segment of mesentery under study in a representative experiment (**Figure 2B**) was also affected by $NaNO_2$ and hypoxic superfusion, presumably due to downstream vasodilation. There was a prolonged increase in BF that persisted for several minutes after 3 min exposure to $NaNO_2$, which was abolished after allopurinol treatment. Capillary perfusion as determined by LDF for this same experiment showed a similar increase with $NaNO_2$ and hypoxia that was attenuated after allopurinol (**Figure 2C**).

We also investigated the role of AOR using raloxifene (2.9–10 mg/kg IP) to inhibit its activity. An example using superfusion with 10 mM $NaNO_2$ in hypoxic and acidic solution is shown in **Figure 3A**, showing vasodilation before treatment (open circles), and complete blocking of the response after raloxifene treatment (solid circles). However, in another experiment shown in **Figure 3B**, treatment with raloxifene did not abolish the vasodilatory response to $NaNO_2$ in hypoxic and acidic solution.

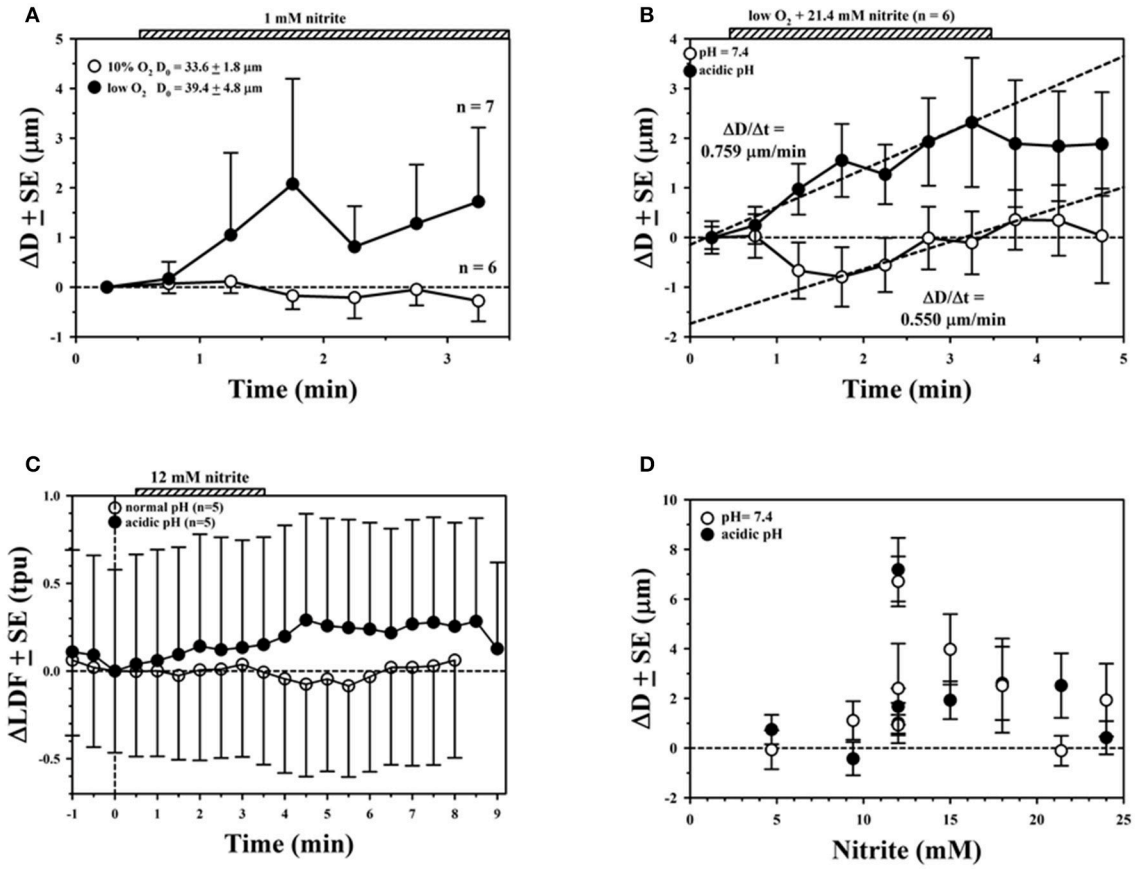

FIGURE 1 | Average ± SE changes in arteriolar diameter (ΔD) measured in rat mesentery during superfusion experiments. **(A)** No effect was seen with 1 mM sodium nitrite ($NaNO_2$) in 10% oxygenated solution (open circles), whereas increases in D were observed with hypoxic solution (solid circles). **(B)** Much larger and more rapid changes in D with $NaNO_2$ were often observed with acidic solution (solid circles) than solution with normal pH (open circles). **(C)** Changes in laser Doppler signal (LDF) showing larger response with acidic superfusion solution. **(D)** Overall ΔD ± SE during superfusion with normal (open circles) or acidic pH (solid circles) over a wide range of $NaNO_2$ concentrations.

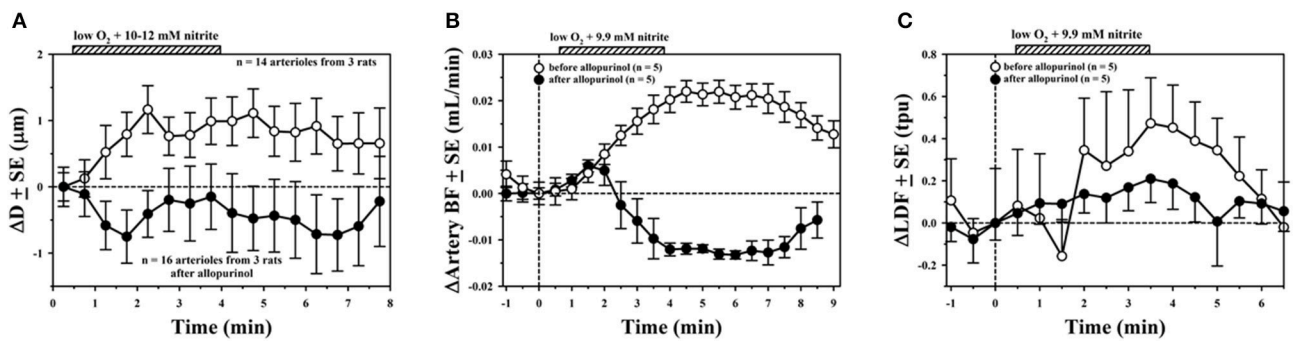

FIGURE 2 | Average ± SE changes before (open circles) and after inhibiting XOR with allopurinol (solid circles) in **(A)** arteriolar diameter, **(B)** small artery blood flow, and **(C)** laser Doppler signal.

In addition to superfusion experiments, we also quantified the effect of $NaNO_2$ delivered to the animal by IP injection. NO microelectrodes were used in these experiments to measure perivascular NO for the arterioles since there was no nitrite in the superfusion solution to interfere with the electrochemical measurement. A representative NO microelectrode measurement is shown in the lower panel of **Figure 4A**. At $t = 0$, the NO microelectrode tip was in

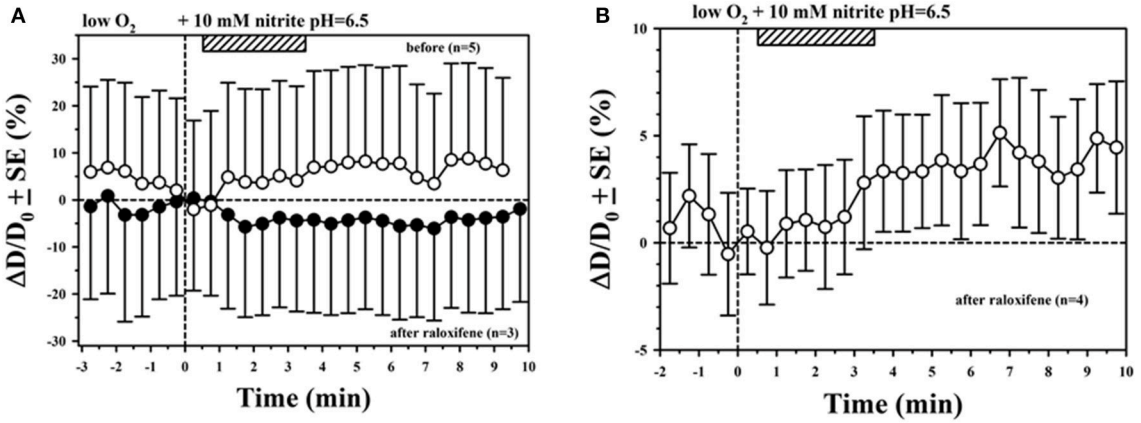

FIGURE 3 | Mixed results for inhibition of AOR with raloxifene. **(A)** Inhibition of vasodilation with superfused $NaNO_2$ was observed in this experiment. **(B)** Vasodilation with superfused $NaNO_2$ was still observed after treating with raloxifene in this experiment.

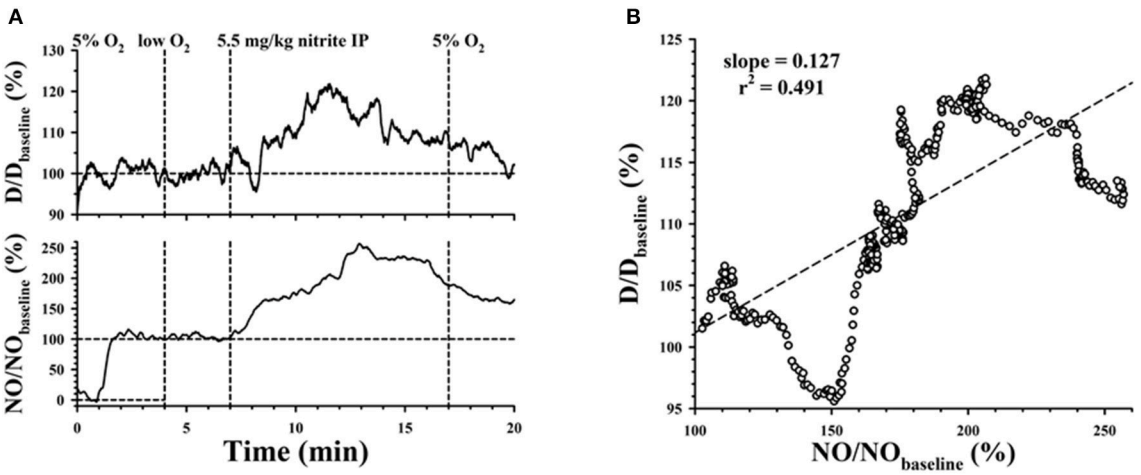

FIGURE 4 | (A) Simultaneous measurements of arteriolar diameter and perivascular NO, normalized by baseline diameter and electrode current. Superfusion was changed from 5% O_2 to low O_2 at $t = 4$ min, then back to 5% O_2 at $t = 17$ min, following an IP injection of $NaNO_2$ at $t = 7$ min. **(B)** Correlation between the normalized perivascular NO and normalized diameter.

the superfusate flowing above the preparation, where there is negligible NO concentration with resulting minimum electrochemical current. The tip was then moved close to the outer surface of the arteriole to measure the baseline perivascular NO, which was used to normalize the measurement. At $t =$ 4 min, the superfusate was changed from a solution with 5% O_2 and 5% CO_2 to a hypoxic solution equilibrated with 0% O_2 and 5% CO_2. At approximately $t = 7$ min, 5.5 mg/kg of $NaNO_2$ was injected IP. Relative changes in diameter, normalized to the baseline diameter, are shown in the upper panel of **Figure 4A**. The peak change in NO occurs about 6 min afterwards, with the peak change in D around 5 min after IP injection. Nevertheless, time courses for the relative changes in NO and D were similar. The correlation between the relative increase in D with NO for normalized data between 7 and 13 min is shown in **Figure 4B**, with positive slope = 0.127%/%. At $t = 17$ min, the superfusion was changed back to oxygenated solution (5% O_2, 5% CO_2) and the arteriolar diameter returned close to baseline, although NO remained elevated for this example. At the end of each measurement, the microelectrode tip was drawn back up into the superfusate to obtain another zero NO current measurement. Any change in the zero NO current from the beginning to the end of the measurement was used to correct for drift, assuming a linear time course.

Further evidence for the role of XOR was found from experiments where nitrite in the bloodstream was increased following IP delivery. Microelectrode measurements confirmed that there was an increase in perivascular NO after IP delivery of $NaNO_2$, which was attenuated after allopurinol. Examples for the time course of relative average changes in diameter (**Figure 5A**) and perivascular NO (**Figure 5B**) for 7 arterioles from 1 rat experiment are shown following IP delivery of 3.4 mg/kg $NaNO_2$

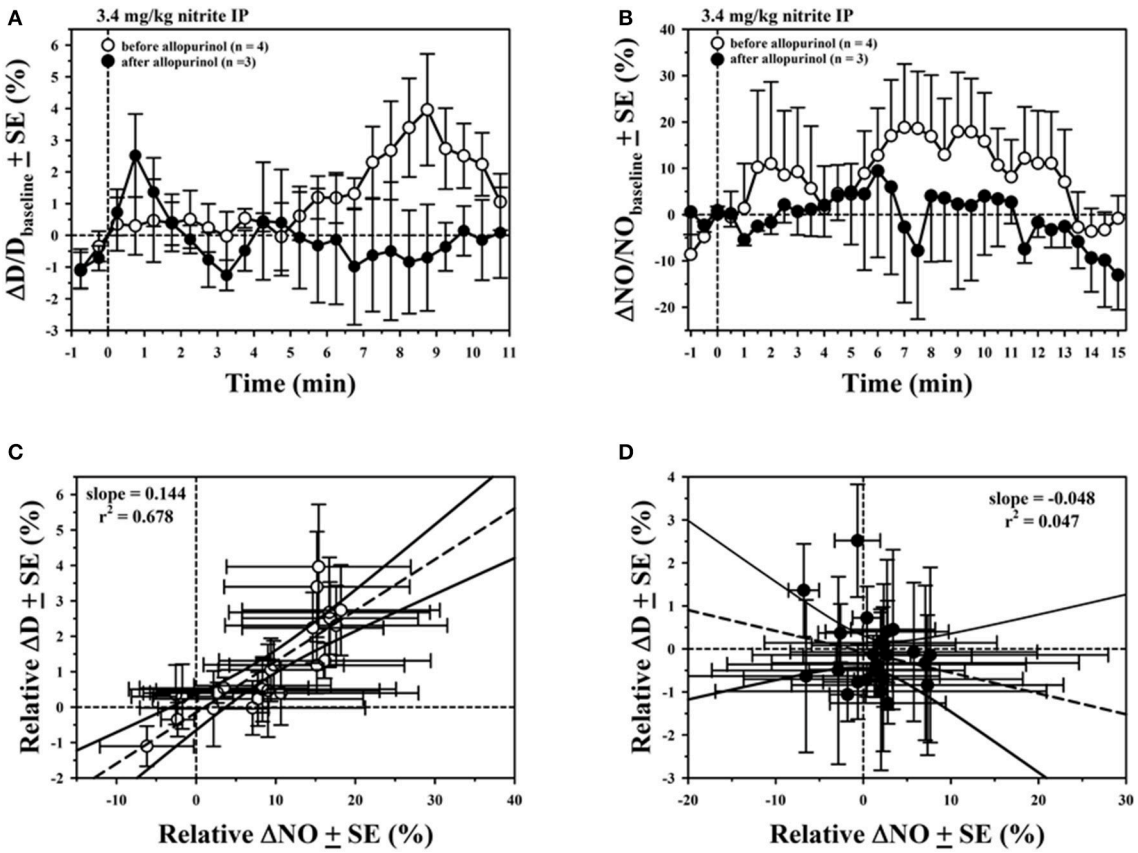

FIGURE 5 | Average ± SE changes in **(A)** normalized arteriolar diameter, **(B)** normalized perivascular NO, following IP injection of $NaNO_2$ at $t = 0$ before (open circles) and after inhibiting XOR with allopurinol (solid circles). Correlations between normalized perivascular NO and normalized diameter are shown **(C)** before and **(D)** after allopurinol.

before and after allopurinol. The ΔD are normalized with respect to the initial diameter ($D_{initial} = 37.0 \pm 1.9\,\mu m$) and ΔNO with respect to the baseline NO level before each nitrite injection. Before allopurinol, the peak change in D after IP injection of $NaNO_2$ occurred around 8.5 min in **Figure 5A**, and around 5 min in **Figure 5B**. There is a significant positive correlation (slope = 0.144%/%) between the normalized average ΔD and ΔNO (**Figure 5C**) with $NaNO_2$ before inhibiting XOR. After a single dose of allopurinol (5 mg/kg IP), there is no longer any correlation (slight negative slope = −0.048%/%, **Figure 5D**). A total of $n = 3$ rat experiments using IP $NaNO_2$ delivery were conducted with allopurinol, and in all three cases, a positive correlation between ΔD and ΔNO was observed before allopurinol ($n = 11$ arterioles) and a negative correlation between ΔD and ΔNO was observed after allopurinol ($n = 9$ arterioles).

Model Predictions

Reducing values for blood PO_2 in the simulation from normoxic (90 Torr) to severely hypoxic levels (10 Torr), predicts a decrease in NO across the computational domain for a baseline case without any generation of NO from nitrite either in blood or tissue (**Figure 6A**). The average NO in the SMC layer decreases monotonically with increasing hypoxia (inset, **Figure 6A**), predicting a 17.1 nM decrease in NO (−29.3%) as blood PO_2 drops from 90 to 10 torr. As reviewed by Gladwin et al. (2009), changes in conformation as hemoglobin becomes deoxygenated results in changes in the rate of nitrite reduction, with a maximum rate in the hypoxic PO_2 range. Our previous simulations (Liu Y. et al., 2016) demonstrate that SMC NO can be significantly elevated through the deoxyhemoglobin nitrite reductase pathway, and further increased in magnitude with increasing nitrite concentration and greater hypoxia. For the case where blood PO_2 drops from 90 to 10 torr, the decrease in SMC NO can be compensated through the deoxyhemoglobin nitrite reductase pathway by increasing the blood nitrite concentration to 284.9 μM (**Figure 6B**).

The effect of tissue XOR nitrite reduction on SMC NO with tissue nitrite = 100 μM was compared against the baseline case (zero nitrite reduction in **Figure 6A**) as a function of blood PO_2 for low (0.03 μM) and high (0.3 μM) concentrations of XOR (**Figures 6C,D**). The contribution to SMC NO from the deoxyhemoglobin nitrite reductase pathway is also shown. NO elevation by XOR has the greatest effect with the highest XOR concentrations at the acidic pH and lowest blood PO_2. For this concentration of nitrite (100 μM), the additional NO is predicted to be +2.4 nM from deoxyhemoglobin nitrite reductase

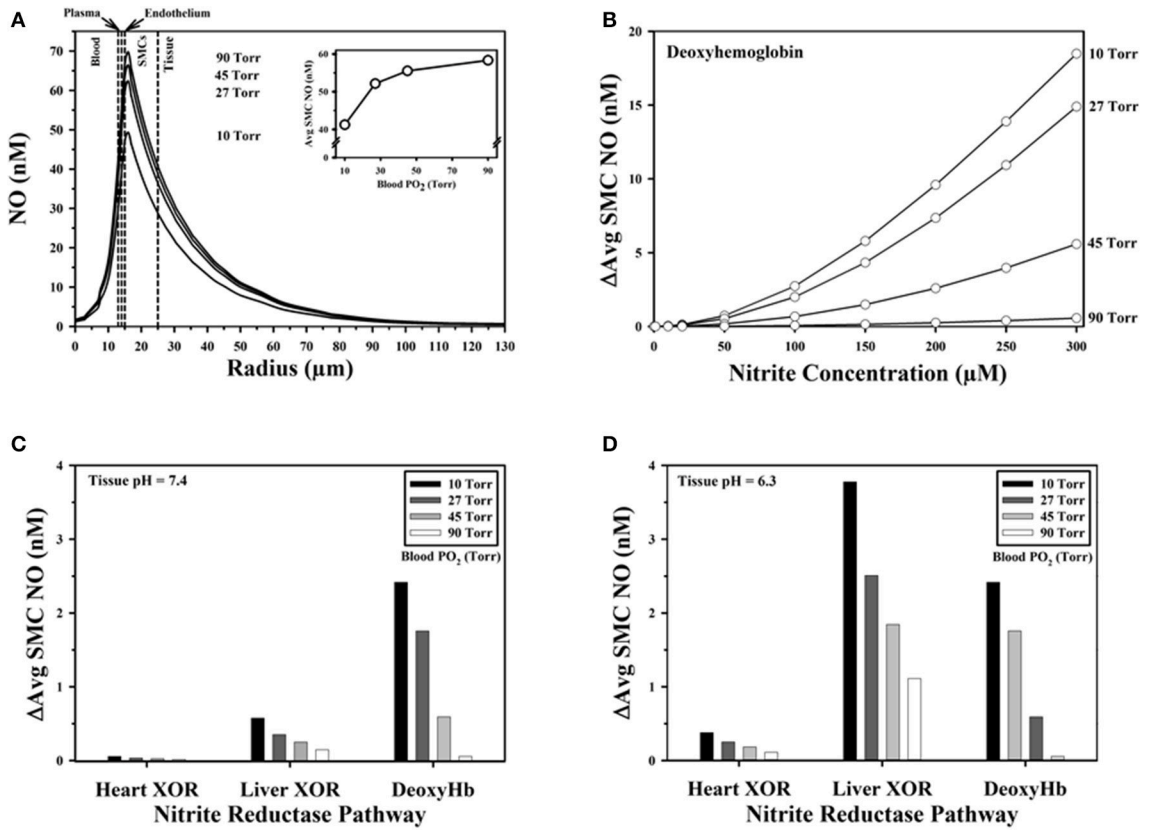

FIGURE 6 | Model predictions. **(A)** Baseline NO concentration profiles across the computational domain predicted for different blood PO_2 values without additional NO released from nitrite. Vertical dashed lines mark boundaries between the five radial model layers. (Inset) Average NO concentration in the smooth muscle cell (SMC) region with decreasing blood PO_2. **(B)** Increase in average SMC NO above baseline predicted with formation of N_2O_3 from deoxyhemoglobin nitrite reductase activity and subsequent release of NO shown as a function of blood PO_2 and nitrite concentration in blood. Effect of low (e.g., in heart) and high (e.g., in liver) tissue nitrite reductase XOR concentrations on elevation of average SMC NO above baseline for **(C)** pH = 7.4 and **(D)** pH = 6.3.

and +3.8 nM from XOR, for a total compensation of +6.2 nM, representing a recovery of 36% from the drop in NO due to the decrease in blood PO_2. The total compensation in NO at pH = 7.4 with the 0.3 μM XOR concentration would be only +3 nM (17.5% recovery), and only +2.47 nM (14.4% recovery) with the lower 0.03 μM XOR concentration. Simulations were also run for the AOR nitrite reductase pathway. AOR has slightly lower reaction rate constants compared with XOR (Maia et al., 2015), and AOR concentrations are generally lower than XOR in the heart and liver (Li et al., 2008). Simulations with AOR predicted ∼10–20% less elevation in SMC NO for pH = 7.4 and 6.3 (not shown).

A sensitivity analysis (**Figure 7**) was conducted for the model parameters listed in **Table 1** to examine the effect of small variations (±5%) in the parameter values on the predicted average SMC NO. Other parameters were held constant for simulations with tissue nitrite = 100 μM, blood PO_2 = 10 Torr, and baseline flow in liver tissue (**Figure 7**). Variations in the concentration of XOR or AOR had the largest effect on the predicted NO, with an intermediate sensitivity to the nitrite diffusion coefficient. The sensitivity was relatively low (<0.1% at +5% variation) for K_mO_2, and the reaction parameters k_{cat} at pH = 7.4. There was a larger effect for variations in the reaction parameter k_{cat} at pH = 6.3 (+0.508% at +5% variation). A 5% increase in the values for $K_mNO_2^-$ at pH = 7.4 and $K_mNO_2^-$ at pH = 6.3 results in small decreases in the SMC NO by −0.079 and −0.385%, respectively.

DISCUSSION

Our *in vivo* results from the rat mesentery microcirculation provide further evidence that nitrite reductases in tissue play a role in increasing NO bioavailability during nitrite-mediated hypoxic vasodilation. We confirmed this by using allopurinol to inhibit XOR (3.4–6 mg/kg IP). Due to time constraints for the *in vivo* experimental procedure, we did not investigate whether a second, higher dose of allopurinol would further inhibit the vasodilatory response. Golwala et al. (2009) used a higher dose of allopurinol (25 mg/kg IV) for their *in vivo* rat studies, and demonstrated that a second 25 mg/kg dose had little further inhibitory effect. They also inhibited AOR using cyanamide (25 mg/kg IV), and alternated the order of inhibitor delivery to discriminate between the contribution of each nitrite

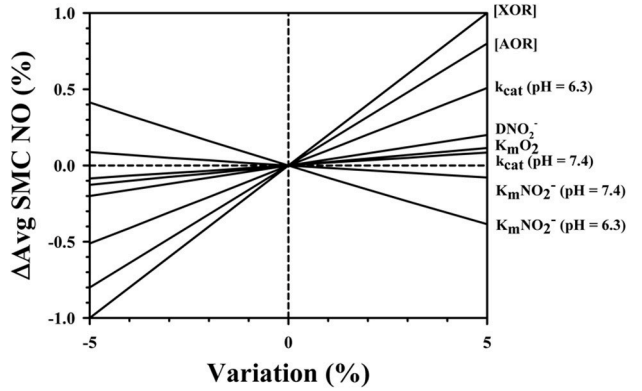

FIGURE 7 | Sensitivity analysis showing the effect of ±5% variations in the model parameters listed in **Table 1** (identified at right of figure) on relative differences in average NO in the SMC region.

reductase on nitrite responses. Nitrite doses of 0.01, 0.03, or 0.1 mM/kg were delivered IV and the changes in systemic blood pressure were measured. Both inhibitors attenuated the decrease in systemic blood pressure with IV delivery of $NaNO_2$. The authors concluded that both XOR and AOR pathways act in parallel in the vasculature.

In our study, we found that it was necessary to use high $NaNO_2$ concentrations (>1 mM in the superfusion solution) to elicit vasodilation (**Figure 1D**). A possible explanation for this finding is that the hypoxic superfusion solution did not significantly lower the blood PO_2 of the arterioles under study, even though we did see a difference (greater vasodilation) with $NaNO_2$ in hypoxic solution compared with $NaNO_2$ in oxygenated solution (**Figure 1A**). The high $NaNO_2$ concentration used in our superfusion experiments is much greater than used for intra-arterial infusions in humans, which demonstrate greater vasodilation under hypoxia than normoxia (Maher et al., 2008). The necessity to use high concentrations of nitrite to generate NO under anoxic conditions *in vitro* was pointed out in the review by Kelley (2015). Consequently, we were not able to directly measure perivascular NO due to electrochemical interference with high nitrite concentrations during superfusion, but we were able to confirm that there was an increase in perivascular NO from the measurements using IP delivery of nitrite. A direct correlation between the increase in NO and vascular diameter was found from these IP injection experiments, which was essentially abolished after inhibiting XOR. The review by Kelley (2015) identifies key factors which allow significant recovery of NO through XOR, including acidic pH and low O_2, as well as other biochemical factors. For example, a recent *in vitro* study using aortic ring preparations and isolated mesenteric arterial bed perfusion found that the nitrate anion (NO_3^-) attenuates XOR-mediated NO generation from nitrite (Damacena-Angelis et al., 2017). To validate the inhibitory effects of nitrate, this study also included experiments with purified XOR using a different inhibitor (febuxostat), which is more potent than allopurinol (Okamoto et al., 2003).

Bryan et al. (2005) studied the time course for uptake and metabolism of nitrite in different organ systems of Wistar rats following IP injection of $NaNO_2$ (range 0.1–10 mg/kg), reporting that tissue nitrite levels were essentially in equilibrium by ∼5 min, when presumably the uptake rate from the abdominal cavity matches the decay rate in blood. Our measurements for the maximum ΔD and ΔNO for the examples shown (**Figures 4A**, **5**) ranged between 5 and 8.5 min. Bryan et al. (2005) reported that nitrate levels as well as the total nitroso/nitrosyl products (RSNO + RNNO + NO-heme) also increased following IP injection of nitrite. We cannot rule out the possibility that some inhibition of the vascular responses by nitrate might occur after repeated IP injections of nitrite in our study as suggested from the results reported by Damacena-Angelis et al. (2017). Bryan et al. (2005) also conducted *in vitro* experiments, and presented evidence that NO formation from nitrite is not required for nitrosation (RSNO) or nitrosylation (RNNO) of thiols, and conclude that these reactions can occur at nitrite concentrations far below that required for vasodilation. A randomized, placebo controlled dose-response study of $NaNO_2$ infusion in humans by Rosenbaek et al. (2017) investigating effects on kidney function and blood pressure found a dose-dependent decrease in urine output with reduced blood pressure. Since they observed no increase in GMP, they concluded that their results supported a direct effect of nitrite or nitrate on the renal tubules and vascular bed with little or no systemic conversion of nitrite to NO.

Many previous studies that have examined the conversion of nitrite to bioactive NO have focused on the role of RBCs through the reductase activity of deoxyhemoglobin (e.g., see Kim-Shapiro and Gladwin, 2014). However, we cannot discriminate whether our experimental results can be specifically attributed to nitrite reductases in blood or tissue (or both). There is strong evidence for greater involvement of tissue nitrite reductases (Feelisch et al., 2008; Li et al., 2008; Arif et al., 2015; Piknova et al., 2015). *In vitro* studies with isolated rabbit aortic rings demonstrate that 10 μM nitrite in the absence of hemoglobin can increase maximal dilation under hypoxic conditions, which can occur with or without the endothelium (Pinder et al., 2009). The authors concluded that AOR, but not XOR, was primarily responsible for nitrite-mediated hypoxic vasorelaxation measured in their study, with some contribution from the cyclooxygenase (COX) pathway. Another *in vitro* study with isolated rat thoracic aorta rings demonstrated attenuation of hypoxic vasorelaxation with nitrite (concentration range from 1 nM to 100 μM) after inhibiting AOR with cyanamide (Arif et al., 2015). We did not get consistent results inhibiting vascular responses to nitrite with raloxifene. We found nitrite-mediated vasodilation was unaffected after raloxifene in one study (**Figure 3B**). Since there is evidence that high concentrations of raloxifene can also inhibit XOR (Weidert et al., 2014), we cannot rule out the possibility that our results showing inhibition of vascular responses with raloxifene (**Figure 3A**) might be due to inhibition of XOR instead of AOR. There might also be vasoactive effects of raloxifene that are independent of NO. We estimated that the raloxifene dose chosen for our studies was not high enough to inhibit XOR. However, it is difficult to discriminate between NO contributions

between XOR and AOR pathways since blocking either pathway depends on inhibitor specificity and dose (Weidert et al., 2014).

It should be recognized that there are other possible mechanisms for the RBC to contribute to hypoxic vasodilation besides the deoxyhemoglobin nitrite reductase-mediated release of NO from nitrite. It has been proposed that the RBC contains a form of eNOS (Kleinbongard et al., 2006), which can produce NO, although it would be subject to immediate scavenging due to the high Hb concentration in the RBC. It has been proposed that formation of Hb(III)NO as an intermediate can account for the majority of NO produced from RBCs (Nagababu et al., 2003). Salgado et al. (2015) propose that this intermediate preferentially locates to the RBC membrane with a greater affinity than Hb. They suggest that a significant amount of NO might be transferred to the vasculature from this pool, avoiding quenching by Hb. Alternately, there is evidence that the RBC releases ATP during hypoxia, which can in turn stimulate NO production by eNOS (Sprague et al., 2007; Cao et al., 2009). We have modeled this effect to predict how ATP can increase shear-stress mediated NO production (Kirby et al., 2016), based on *in vitro* NO measurements with cultured ECs (Andrews et al., 2014). Another proposed mechanism is the formation of S-nitrosohemoglobin (SNO-Hb), as reviewed by Singel and Stamler (2005). However, there is contradictory evidence for this mechanism (Isbell et al., 2008). Furthermore, a mathematical model by Chen K. et al. (2007) did not predict a significant NO contribution from this pathway.

There are also other mechanisms in tissue beside nitrite reductases that can contribute NO during hypoxia, as reviewed by Buerk (2007) and Kim-Shapiro and Gladwin (2014). There is evidence that cytochrome c in the mitochondria can be a source of NO by reducing nitrite (Kozlov et al., 1999). It has also been proposed that there is a mitochondrial form of NOS (mtNOS) that can produce NO, although the existence of mtNOS is questioned (Lacza et al., 2006). NO or related reactive species can modify tissue proteins, forming *S*-nitrosothiols, *S*-nitrosoalbumin, and other *S*-nitrosoprotein species under normal physiological conditions which might serve as a storage pool in tissue for NO or other vasoactive species (Jourd'heuil et al., 2000; Liu T. et al., 2016). On the other hand, these reactions may modify vascular tone signaling pathways independently from any NO recovered from nitrite. While normally myoglobin is a strong scavenger of NO, it is recognized that myoglobin can also cause nitrite bioactivation by reducing nitrite (Shiva et al., 2007; Totzeck et al., 2012, 2014; Piknova et al., 2015). We have developed a mathematical model for a cardiac arteriole and surrounding myocardium (Liu et al., 2017), showing how myoglobin functions as a nitrite reductase to elevate SMC NO during hypoxia in an O_2- and pH-dependent manner.

Limitations of Mathematical Model

Our simulations assume that published reaction parameters (Maia and Moura, 2011; Maia et al., 2015) were constant with abundant substrate, and were only affected by changing O_2 or pH levels. The model assumes that all N_2O_3 homolyzes to NO, ignoring other nitrosation reactions that are known to occur (Basu et al., 2007; Kim-Shapiro and Gladwin, 2014), thus we may be overestimating the increase in SMC NO. It is also possible, as suggested by Koppenol (2012) and Tu et al. (2009), that it is not energetically possible for the reactions to generate N_2O_3 to occur. As with any computer simulation, the accuracy of model parameters determines whether the predictions are physiologically relevant. The measurement of reaction rates is hindered by experimental difficulties and complex interactions among XOR, AOR, nitrite, nitrate, and NO (Jourd'heuil et al., 2000; Maia and Moura, 2011; Cantu-Medellin and Kelley, 2013; Damacena-Angelis et al., 2017). The concentration of nitrite reductase enzymes in tissue is not well-characterized and may not be uniformly distributed. We are not aware of any estimates for the enzyme concentrations and reaction parameters in mesentery. Future simulations would be necessary if more precise information about reaction rates, localized spatial distributions, and concentrations become available. The predicted changes in SMC NO with physiologically relevant nitrite concentrations in the 0.2–2 μM range are quite small ($<$1 nM) even for hypoxic conditions. Even with much higher nitrite levels (up to 300 μM), the increase in SMC NO predicted for the deoxyhemoglobin nitrite reductase pathway is $<$20 nM during severe hypoxia with blood $PO_2 = 10$ torr (**Figure 6B**).

In conclusion, our *in vivo* experimental results are consistent with other studies that suggest that the reduction of nitrite through the activity of tissue nitrite reductases can contribute NO to vascular smooth muscle to enhance hypoxic vasodilation. However, it is difficult to assess whether hypoxic vasodilation can be specifically attributed to nitrite reductase activity in blood or tissue, or both. It is also very difficult to experimentally create the severe *in vivo* physiological conditions for maximal effects. Our theoretical model demonstrates that is possible to compensate for the loss of NO production by eNOS during hypoxia by all three pathways: deoxyhemoglobin nitrite reductase in RBCs, and the tissue nitrite reductases XOR and AOR. This modeling approach can be further developed to explore other biochemical pathways that can contribute NO or other nitrogen species that enhance hypoxic vasodilation.

AUTHOR CONTRIBUTIONS

DB was responsible for the experimental design, conducting animal research, data analysis, model development, writing and editing the paper. YL was responsible for computer simulations and contributed written content. KZ assisted with animal surgery and editing the paper. KB and DJ were responsible for model development and editing the paper.

FUNDING

Supported by HL 116256 from NIH.

REFERENCES

Andrews, A. M., Jaron, D., Buerk, D. G., and Barbee, K. A. (2014). Shear stress-induced NO production is dependent on ATP autocrine signaling and capacitative calcium entry. *Cell Mol. Bioeng.* 7, 510–520. doi: 10.1007/s12195-014-0351-x

Arif, S., Borgognone, A., Lin, E. L., O'Sullivan, A. G., Sharma, V., Drury, N. E., et al. (2015). Role of aldehyde dehydrogenase in hypoxic vasodilator effects of nitrite in rats and humans. *Br. J. Pharmacol.* 172, 3341–3352. doi: 10.1111/bph.13122

Azizi, F., Kielbasa, J. E., Adeyiga, A. M., Maree, R. D., Frazier, M., Yakubu, M., et al. (2005). Rates of nitric oxide dissociation from hemoglobin. *Free Radic. Biol. Med.* 39, 145–151. doi: 10.1016/j.freeradbiomed.2005.03.001

Basu, S., Grubina, R., Huang, J., Conradie, J., Huang, Z., Jeffers, A., et al. (2007). Catalytic generation of N_2O_3 by the concerted nitrite reductase and anhydrase activity of hemoglobin. *Nat. Chem. Biol.* 3, 785–794. doi: 10.1038/nchembio.2007.46

Blood, A. B. (2017). The medicinal chemistry of nitrite as a source of nitric oxide signaling. *Curr. Top Med. Chem.* 17, 1758–1768. doi: 10.2174/1568026617666161116145046

Bonner, R. F., Clem, T. R., Bowen, P. D., and Bowman, R. L. (1981). "Laser-doppler continuous real-time monitor of pulsatile and mean blood flow," in *Tissue Microcirculation. Scattering Techniques Applied to Supra-Molecular and Nonequilibrium Systems*, eds S. H. Chen, B. Chu, and R. Nossal (New York, NY: Plenum), 685–702.

Bryan, N. S., Fernandez, B. O., Bauer, S. M., Garcia-Saura, M. F., Milsom, A. B., Rassaf, T., et al. (2005). Nitrite is a signaling molecule and regulator of gene expression in mammalian tissues. *Nat. Chem. Biol.* 1, 290–297. doi: 10.1038/nchembio734

Buerk, D. G. (2007). Nitric oxide regulation of microvascular oxygen. *Antioxid. Redox Signal.* 9, 829–843. doi: 10.1089/ars.2007.1551

Buerk, D. G., Barbee, K. A., and Jaron, D. (2011a). Modeling O_2-dependent effects of nitrite reductase activity in blood and tissue on coupled NO and O_2 transport around arterioles. *Adv. Exp. Med. Biol.* 701, 271–276. doi: 10.1007/978-1-4419-7756-4_36

Buerk, D. G., Barbee, K. A., and Jaron, D. (2011b). Nitric oxide signaling in the microcirculation. *Crit. Rev. Biomed. Eng.* 39, 397–433. doi: 10.1615/CritRevBiomedEng.v39.i5.40

Buerk, D. G., Lamkin-Kennard, K., and Jaron, D. (2003). Modeling the influence of superoxide dismutase on superoxide and nitric oxide interactions, including reversible inhibition of oxygen consumption. *Free Radic. Biol. Med.* 34, 1488–1503. doi: 10.1016/S0891-5849(03)00178-3

Butler, A. R., and Ridd, J. H. (2004). Formation of nitric oxide from nitrous acid in ischemic tissue and skin. *Nitric Oxide* 10, 20–24. doi: 10.1016/j.niox.2004.01.004

Cantu-Medellin, N., and Kelley, E. E. (2013). Xanthine oxidoreductase-catalyzed reduction of nitrite to nitric oxide: insights regarding where, when and how. *Nitric Oxide* 34, 19–26. doi: 10.1016/j.niox.2013.02.081

Cao, Z., Bell, J. B., Mohanty, J. G., Nagababu, E., and Rifkind, J. M. (2009). Nitrite enhances RBC hypoxic ATP synthesis and the release of ATP into the vasculature: a new mechanism for nitrite-induced vasodilation. *Am. J. Physiol. Heart Circ. Physiol.* 297, H1494–H1503. doi: 10.1152/ajpheart.01233.2008

Chen, K., Piknova, B., Pittman, R. N., Schechter, A. N., and Popel, A. S. (2008). Nitric oxide from nitrite reduction by hemoglobin in the plasma and erythrocytes. *Nitric Oxide* 18, 47–60. doi: 10.1016/j.niox.2007.09.088

Chen, K., Pittman, R. N., and Popel, A. S. (2007). Vascular smooth muscle NO exposure from intraerythrocytic SNOHb: a mathematical model. *Antioxid. Redox Signal.* 9, 1097–1110. doi: 10.1089/ars.2007.1594

Chen, X., Buerk, D. G., Barbee, K. A., and Jaron, D. (2007). A model of NO/O_2 transport in capillary-perfused tissue containing an arteriole and venule pair. *Ann. Biomed. Eng.* 35, 517–529. doi: 10.1007/s10439-006-9236-z

Chen, X., Jaron, D., Barbee, K. A., and Buerk, D. G. (2006). The influence of radial RBC distribution, blood velocity profiles, and glycocalyx on coupled NO/O_2 transport. *J. Appl. Physiol.* 100, 482–492. doi: 10.1152/japplphysiol.00633.2005

Cosby, K., Partovi, K. S., Crawford, J. H., Patel, R. P., Reiter, C. D., Martyr, S., et al. (2003). Nitrite reduction to nitric oxide by deoxyhemoglobin vasodilates the human circulation. *Nat. Med.* 9, 1498–1505. doi: 10.1038/nm954

Damacena-Angelis, C., Oliveira-Paula, G. H., Pinheiro, L. C., Crevelin, E. J., Portella, R. L., Moraes, L. A. B., et al. (2017). Nitrate decreases xanthine oxidoreductase-mediated nitrite reductase activity and attenuates vascular and blood pressure responses to nitrite. *Redox. Biol.* 12, 291–299. doi: 10.1016/j.redox.2017.03.003

Dejam, A., Hunter, C. J., Tremonti, C., Pluta, R. M., Hon, Y. Y., Grimes, G., et al. (2007). Nitrite infusion in humans and nonhuman primates: endocrine effects, pharmacokinetics, and tolerance formation. *Circulation* 116, 1821–1831. doi: 10.1161/CIRCULATIONAHA.107.712133

Feelisch, M., Fernandez, B. O., Bryan, N. S., Garcia-Saura, M. F., Bauer, S., Whitlock, D. R., et al. (2008). Tissue processing of nitrite in hypoxia: an intricate interplay of nitric oxide-generating and -scavenging systems. *J. Biol. Chem.* 283, 33927–33934. doi: 10.1074/jbc.M806654200

Gladwin, M. T. (2008). Evidence mounts that nitrite contributes to hypoxic vasodilation in the human circulation. *Circulation* 117, 594–597. doi: 10.1161/CIRCULATIONAHA.107.753897

Gladwin, M. T., Grubina, R., and Doyle, M. P. (2009). The new chemical biology of nitrite reactions with hemoglobin: R-state catalysis, oxidative denitrosylation, and nitrite reductase/anhydrase. *Acc. Chem. Res.* 42, 157–167. doi: 10.1021/ar800089j

Golwala, N. H., Hodenette, C., Murthy, S. N., Nossaman, B. D., and Kadowitz, P. J. (2009). Vascular responses to nitrite are mediated by xanthine oxidoreductase and mitochondrial aldehyde dehydrogenase in the rat. *Can. J. Physiol. Pharmacol.* 87, 1095–1101. doi: 10.1139/Y09-101

Helms, C. C., Liu, X., and Kim-Shapiro, D. B. (2017). Recent insights into nitrite signaling processes in blood. *Biol. Chem.* 398, 319–329. doi: 10.1515/hsz-2016-0263

Hopmann, K. H., Cardey, B., Gladwin, M. T., Kim-Shapiro, D. B., and Ghosh, A. (2011). Hemoglobin as a nitrite anhydrase: modeling methemoglobin-mediated N2O3 formation. *Chemistry* 17, 6348–6358. doi: 10.1002/chem.201003578

Isbell, T. S., Sun, C. W., Wu, L. C., Teng, X., Vitturi, D. A., Branch, B. G., et al. (2008). SNO-hemoglobin is not essential for red blood cell-dependent hypoxic vasodilation. *Nat. Med.* 14, 773–777. doi: 10.1038/nm1771

Jourd'heuil, D., Hallen, K., Feelisch, M., and Grisham, M. B. (2000). Dynamic state of S-nitrosothiols in human plasma and whole blood. *Free Radic. Biol. Med.* 28, 409–417. doi: 10.1016/S0891-5849(99)00257-9

Kelley, E. E. (2015). A new paradigm for XOR-catalyzed reactive species generation in the endothelium. *Pharmacol. Rep.* 67, 669–674. doi: 10.1016/j.pharep.2015.05.004

Kevil, C. G., Kolluru, G. K., Pattillo, C. B., and Giordano, T. (2011). Inorganic nitrite therapy: historical perspective and future directions. *Free Radic. Biol. Med.* 51, 576–593. doi: 10.1016/j.freeradbiomed.2011.04.042

Kim-Shapiro, D. B., and Gladwin, M. T. (2014). Mechanisms of nitrite bioactivation. *Nitric Oxide* 38, 58–68. doi: 10.1016/j.niox.2013.11.002

Kirby, P. L., Buerk, D. G., Parikh, J., Barbee, K. A., and Jaron, D. (2016). Mathematical model for shear stress dependent NO and adenine nucleotide production from endothelial cells. *Nitric Oxide* 52, 1–15. doi: 10.1016/j.niox.2015.10.004

Kleinbongard, P., Schulz, R., Rassaf, T., Lauer, T., Dejam, A., Jax, T., et al. (2006). Red blood cells express a functional endothelial nitric oxide synthase. *Blood* 107, 2943–2951. doi: 10.1182/blood-2005-10-3992

Koppenol, W. H. (2012). Nitrosation, thiols, and hemoglobin: energetics and kinetics. *Inorg. Chem.* 51, 5637–5641. doi: 10.1021/ic202561f

Kozlov, A. V., Staniek, K., and Nohl, H. (1999). Nitrite reductase activity is a novel function of mammalian mitochondria. *FEBS Lett.* 454, 127–130. doi: 10.1016/S0014-5793(99)00788-7

Lacza, Z., Pankotai, E., Csordas, A., Gero, D., Kiss, L., Horvath, E. M., et al. (2006). Mitochondrial, N. O., and reactive nitrogen species production: does mtNOS exist? *Nitric Oxide* 14, 162–168. doi: 10.1016/j.niox.2005.05.011

Lamkin-Kennard, K. A., Buerk, D. G., and Jaron, D. (2004a). Interactions between NO and O_2 in the microcirculation: a mathematical analysis. *Microvasc. Res.* 68, 38–50. doi: 10.1016/j.mvr.2004.03.001

Lamkin-Kennard, K. A., Jaron, D., and Buerk, D. G. (2004b). Impact of the fahraeus effect on NO and O_2 biotransport: a computer model. *Microcirculation* 11, 337–349. doi: 10.1080/10739680490437496

Li, H., Cui, H., Kundu, T. K., Alzawahra, W., and Zweier, J. L. (2008). Nitric oxide production from nitrite occurs primarily in tissues not in the blood: critical role of xanthine oxidase and aldehyde oxidase. *J. Biol. Chem.* 283, 17855–17863. doi: 10.1074/jbc.M801785200

Liu, T., Schroeder, H. J., Wilson, S. M., Terry, M. H., Romero, M., Longo, L. D., et al. (2016). Local and systemic vasodilatory effects of low molecular weight S-nitrosothiols. *Free Radic. Biol. Med.* 91, 215–223. doi: 10.1016/j.freeradbiomed.2015.12.009

Liu, Y., Buerk, D. G., Barbee, K. A., and Jaron, D. (2016). A mathematical model for the role of N_2O_3 in enhancing nitric oxide bioavailability following nitrite infusion. *Nitric Oxide* 60, 1–9. doi: 10.1016/j.niox.2016.08.003

Liu, Y., Buerk, D. G., Barbee, K. A., and Jaron, D. (2017). Nitric oxide release by deoxymyoglobin nitrite reduction during cardiac ischemia: a mathematical model. *Microvasc. Res.* 112, 79–86. doi: 10.1016/j.mvr.2017.03.009

Lloyd, N. L. (1957). A new kit for sodium nitrite-thiosulphate therapy in the treatment of acute cyanide poisoning. *Br. J. Ind. Med.* 14:137. doi: 10.1136/oem.14.2.137

MacArthur, P. H., Shiva, S., and Gladwin, M. T. (2007). Measurement of circulating nitrite and S-nitrosothiols by reductive chemiluminescence. *J. Chromatogr. B Analyt. Technol. Biomed. Life Sci.* 851, 93–105. doi: 10.1016/j.jchromb.2006.12.012

Maher, A. R., Milsom, A. B., Gunaruwan, P., Abozguia, K., Ahmed, I., Weaver, R. A., et al. (2008). Hypoxic modulation of exogenous nitrite-induced vasodilation in humans. *Circulation* 117, 670–677. doi: 10.1161/CIRCULATIONAHA.107.719591

Maia, L. B., and Moura, J. J. (2011). Nitrite reduction by xanthine oxidase family enzymes: a new class of nitrite reductases. *J. Biol. Inorg. Chem.* 16, 443–460. doi: 10.1007/s00775-010-0741-z

Maia, L. B., Pereira, V., Mira, L., and Moura, J. J. (2015). Nitrite reductase activity of rat and human xanthine oxidase, xanthine dehydrogenase, and aldehyde oxidase: evaluation of their contribution to NO formation *in vivo*. *Biochemistry* 54, 685–710. doi: 10.1021/bi500987w

Nagababu, E., Ramasamy, S., Abernethy, D. R., and Rifkind, J. M. (2003). Active nitric oxide produced in the red cell under hypoxic conditions by deoxyhemoglobin-mediated nitrite reduction. *J. Biol. Chem.* 278, 46349–46356. doi: 10.1074/jbc.M307572200

Neild, T. O. (1989). Measurement of arteriole diameter changes by analysis of television images. *Blood Vessels* 26, 48–52.

Okamoto, K., Eger, B. T., Nishino, T., Kondo, S., Pai, E. F., and Nishino, T. (2003). An extremely potent inhibitor of xanthine oxidoreductase. crystal structure of the enzyme-inhibitor complex and mechanism of inhibition. *J. Biol. Chem.* 278, 1848–1855. doi: 10.1074/jbc.M208307200

Omar, S. A., Webb, A. J., Lundberg, J. O., and Weitzberg, E. (2016). Therapeutic effects of inorganic nitrate and nitrite in cardiovascular and metabolic diseases. *J. Intern. Med.* 279, 315–336. doi: 10.1111/joim.12441

Piknova, B., Park, J. W., Swanson, K. M., Dey, S., Noguchi, C. T., and Schechter, A. N. (2015). Skeletal muscle as an endogenous nitrate reservoir. *Nitric Oxide* 47, 10–16. doi: 10.1016/j.niox.2015.02.145

Pinder, A. G., Pittaway, E., Morris, K., and James, P. E. (2009). Nitrite directly vasodilates hypoxic vasculature via nitric oxide-dependent and -independent pathways. *Br. J. Pharmacol.* 157, 1523–1530. doi: 10.1111/j.1476-5381.2009.00340.x

Pinotti, A., Graiver, N., Califano, A., and Zaritzky, N. (2002). Diffusion of nitrite and nitrate salts in pork tissue in the presence of sodium chloride. *J. Food Sci.* 67, 2165–2171. doi: 10.1111/j.1365-2621.2002.tb09521.x

Pluta, R. M., Oldfield, E. H., Bakhtian, K. D., Fathi, A. R., Smith, R. K., Devroom, H. L., et al. (2011). Safety and feasibility of long-term intravenous sodium nitrite infusion in healthy volunteers. *PLoS ONE* 6:e14504. doi: 10.1371/journal.pone.0014504

Ray, R., and Shah, A. M. (2005). NADPH oxidase and endothelial cell function. *Clin. Sci.* 109, 217–226. doi: 10.1042/CS20050067

Reichert, E. T., and Mitchell, S. W. (1880). On the physiological action of potassium nitrite. *Am. J. Med. Sci.* 156, 158–180. doi: 10.1097/00000441-188007000-00011

Rong, Z., Alayash, A. I., Wilson, M. T., and Cooper, C. E. (2013a). Modulating hemoglobin nitrite reductase activity through allostery: a mathematical model. *Nitric Oxide* 35, 193–198. doi: 10.1016/j.niox.2013.10.007

Rong, Z., Wilson, M. T., and Cooper, C. E. (2013b). A model for the nitric oxide producing nitrite reductase activity of hemoglobin as a function of oxygen saturation. *Nitric Oxide* 33, 74–80. doi: 10.1016/j.niox.2013.06.008

Rosenbaek, J. B., Al Therwani, S., Jensen, J. M., Mose, F. H., Wandall-Frostholm, C., Pedersen, E. B., et al. (2017). Effect of sodium nitrite on renal function and sodium and water excretion and brachial and central blood pressure in healthy subjects: a dose-response study. *Am. J. Physiol. Renal. Physiol.* 313, F378–F387. doi: 10.1152/ajprenal.00400.2016

Salgado, M. T., Cao, Z., Nagababu, E., Mohanty, J. G., and Rifkind, J. M. (2015). Red blood cell membrane-facilitated release of nitrite-derived nitric oxide bioactivity. *Biochemistry* 54, 6712–6723. doi: 10.1021/acs.biochem.5b00643

Shiva, S., Huang, Z., Grubina, R., Sun, J., Ringwood, L. A., MacArthur, P. H., et al. (2007). Deoxymyoglobin is a nitrite reductase that generates nitric oxide and regulates mitochondrial respiration. *Circ. Res.* 100, 654–661. doi: 10.1161/01.RES.0000260171.52224.6b

Singel, D. J., and Stamler, J. S. (2005). Chemical physiology of blood flow regulation by red blood cells: the role of nitric oxide and S-nitrosohemoglobin. *Annu. Rev. Physiol.* 67, 99–145. doi: 10.1146/annurev.physiol.67.060603.090918

Smith, R. P., and Gosselin, R. E. (1979). Hydrogen sulfide poisoning. *J. Occup. Med.* 21, 93–97. doi: 10.1097/00043764-197902000-00008

Sprague, R. S., Stephenson, A. H., and Ellsworth, M. L. (2007). Red not dead: signaling in and from erythrocytes. *Trends Endocrinol. Metab.* 18, 350–355. doi: 10.1016/j.tem.2007.08.008

Totzeck, M., Hendgen-Cotta, U. B., Kelm, M., and Rassaf, T. (2014). Crosstalk between nitrite, myoglobin and reactive oxygen species to regulate vasodilation under hypoxia. *PLoS ONE* 9:e105951. doi: 10.1371/journal.pone.0105951

Totzeck, M., Hendgen-Cotta, U. B., Luedike, P., Berenbrink, M., Klare, J. P., Steinhoff, H. J., et al. (2012). Nitrite regulates hypoxic vasodilation via myoglobin-dependent nitric oxide generation. *Circulation* 126, 325–334. doi: 10.1161/CIRCULATIONAHA.111.087155

Tu, C., Mikulski, R., Swenson, E. R., and Silverman, D. N. (2009). Reactions of nitrite with hemoglobin measured by membrane inlet mass spectrometry. *Free Radic. Biol. Med.* 46, 14–19. doi: 10.1016/j.freeradbiomed.2008.09.016

van Faassen, E. E., Bahrami, S., Feelisch, M., Hogg, N., Kelm, M., Kim-Shapiro, D. B., et al. (2010). Nitrite as regulator of hypoxic signaling in mammalian physiology. *Med. Res. Rev.* 29, 683–741. doi: 10.1002/med.20151

Webb, A. J., Milsom, A. B., Rathod, K. S., Chu, W. L., Qureshi, S., Lovell, M. J., et al. (2008). Mechanisms underlying erythrocyte and endothelial nitrite reduction to nitric oxide in hypoxia: role for xanthine oxidoreductase and endothelial nitric oxide synthase. *Circ. Res.* 103, 957–964. doi: 10.1161/CIRCRESAHA.108.175810

Weidert, E. R., Schoenborn, S. O., Cantu-Medellin, N., Choughule, K. V., Jones, J. P., and Kelley, E. E. (2014). Inhibition of xanthine oxidase by the aldehyde oxidase inhibitor raloxifene: implications for identifying molybdopterin nitrite reductases. *Nitric Oxide* 37, 41–45. doi: 10.1016/j.niox.2013.12.010

Weiss, S., Wilkins, R. W., and Haynes, F. W. (1937). The nature of circulatory collapse induced by sodium nitrite. *J. Clin. Invest.* 16, 73–84. doi: 10.1172/JCI100840

Wilkins, R. W., Haynes, F. W., and Weiss, S. (1937). The role of the venous system in circulatory collapse induced by sodium nitrite. *J. Clin. Invest.* 16, 85–91. doi: 10.1172/JCI100841

Conflict of Interest Statement: The authors declare that the research was conducted in the absence of any commercial or financial relationships that could be construed as a potential conflict of interest.